AIAA JOURNAL
Vol. 46, No. 3, March 2008

Technical Notes

TECHNICAL NOTES are short manuscripts describing new developments or important results of a preliminary nature. These Notes should not exceed 2500 words (where a figure or table counts as 200 words). Following informal review by the Editors, they may be published within a few months of the date of receipt. Style requirements are the same as for regular contributions (see inside back cover).

Spinning Projectile with an Inviscid Liquid Payload Impregnating Porous Media

G. R. Cooper*
U.S. Army Research Laboratory,
Aberdeen Proving Ground, Maryland 21005-5069

DOI: 10.2514/1.30481

Nomenclature

a	=	radius of cylinder containing fluid
C	=	half-length of the cylinder containing N subcylinders
C_t	=	radial and azimuthal porosity coefficient
C_x	=	axial porosity coefficient
f_j	=	$1 + 2\pi a^4 C\rho / I_x C_{\mathrm{LIM}j}$
$\mathbf{J}$, $\mathbf{K}$	=	Cartesian unit vectors
$\hat{K}$	=	coning angle
m_L	=	liquid mass, $2\pi a^2 C\rho$
N	=	number of subcylinders per candlestick
P	=	projectile angular velocity along the X_E axis
$\hat{p}$	=	liquid pressure perturbation
$\boldsymbol{q}$	=	liquid velocity vector
$\mathbf{R}$	=	position vector
S	=	complex coning frequency, $(\varepsilon + i)T$
S_g	=	gyroscopic stability factor
T, T_j	=	nondimensionalized coning frequencies
t	=	time
u, v, w	=	liquid perturbation axial, radial, and azimuthal velocity components
Δ	=	subcylinder length, $2C/N$
ε, ε_j	=	growth rates per cycle
ε_{aj}	=	growth rate per cycle due to aerodynamic moment
κ_t, κ_x	=	transverse and axial pore sizes of the porous matrix (dimensions of lengths squared)
μ	=	dynamic viscosity of liquid
ρ	=	liquid mass density
ϕ_j	=	$\phi_{j0} + T_j P t$

Introduction

PREDICTING the angular motion induced by a liquid payload contained in a coning projectile has been of considerable interest to the U. S. Army. The addition of liquid moments acting on these projectiles has displayed catastrophic flight instabilities in their pitching and yawing motions. An examination of this phenomenon by Stewartson [1] made a theoretical study of a spinning top containing an inviscid liquid in a right circular cylinder. His analysis used the linearized Euler equations to predict liquid moments for a top undergoing circular or spiral motion. A spectrum of spin eigenfrequencies determined when the liquid moments become infinite. Such moments indicate spin frequencies at which instabilities are likely to occur.

To better understand the physics of liquid moments, many authors have applied both high- and low-viscosity corrections to the Stewartson [1] theory when examining liquids in coning projectiles [2–6]. Generally, these corrections use the linearized Navier–Stokes equations and/or singular boundary-layer theory to account for viscosity. The interested reader can find details of these methods in the given references.

Projectiles with liquid payloads saturating highly permeable material have also interested the Army. One reason for using permeable media is to reduce the spin-up time of the contained liquid [7]. Saturated permeable media also causes better payload dispersion when the projectile impacts a target. However, flight stability for these payloads has been an issue in flight test experiments conducted by D'Amico and Clay [8]. An analytical investigation by Cooper [9] examined the liquid moments acting on a projectile housing an inviscid liquid saturating porous media. This investigation assumed that the porosity is uniform in all directions. The analysis also considered the payload to consist of one or more cylinders stacked end to end along the projectile symmetry axis separated by impermeable endcaps.

The present work extends Cooper's [9] theory by allowing the porosity in the axial direction to differ from the porosities in the lateral directions. The reason for this added feature is that many porous materials used to construct liquid-filled projectiles do not have porosities identical in all directions. In particular, many porous materials have porosity in the axial direction that is different from the porosity in the orthogonal directions. Following the previous report [9], the projectile payload cavity is again segmented along the projectile symmetry axis into a sequence of equal-length cylinders and each cylinder is separated by impermeable endcaps. Moments caused by the saturated porous media are calculated using a simple modification of the well-established linearized Euler equations [1]. This modification assumes that flow through porous media is accounted for by adding terms to the linearized Euler equations [9]. These terms are proportional to the porosity of the porous matrix and the liquid velocity relative to this matrix, which is taken to be rigidly attached to the projectile. The following analysis examines induced payload moments and the possibility of large overturning moments due to resonances. These moments are presented as functions of the payload geometry and media porosities for typical coning frequencies of the free-flight projectiles.

Projectile Dynamics

The projectile dynamics in this paper parallel the dynamics given by Murphy [3], such that X, Y, and Z and X, $\tilde{Y}$, and $\tilde{Z}$ are, respectively, body and nonrolling coordinate systems, where the X axis is the projectile's symmetry axis. The Earth-fixed axes X_E, Y_E, and Z_E have X_E initially along the velocity vector, and $\tilde{Z}$ and Z_E are initially downward, so that a unit vector along X has Earth-fixed components n_{XE}, n_{YE}, and n_{ZE}. The angle of attack $\tilde{\alpha}$ in the nonrolling system is the angle from the velocity vector to X projected

Received 15 February 2007; revision received 10 July 2007; accepted for publication 2 October 2007.

*Research Physicist, Weapons and Materials Research Directorate. Member AIAA.

onto the X–$\tilde{Z}$ plane, and the angle of sideslip $\tilde{\beta}$ is the angle in the X–$\tilde{Y}$ plane from X to the velocity vector.

Linear projectile theory [10] gives a second-order differential equation for $\tilde{\xi} = \tilde{\beta} + i\tilde{\alpha}$, and the solution is an epicycle with the form

$$\tilde{\xi} = K_1 e^{iT_1 Pt} + K_2 e^{iT_2 Pt} \tag{1}$$

where

$$\ell_n(K_j/K_{j0}) = \varepsilon_j T_j P t \qquad T_j = \sigma/2[1 \pm \sqrt{1 - 1/S_g}] \tag{2}$$

Moments due to the liquid payload are assumed to be caused by the coning motions of Eq. (1), and the linear response of these moments is modeled as [3]

$$M_{L\tilde{Y}} + iM_{L\tilde{Z}} = m_L a^2 P^2 [T_1 C_{\mathrm{LM}_1} K_1 e^{i\phi_1} + T_2 C_{\mathrm{LM}_2} K_2 e^{i\phi_2}] \tag{3}$$

C_{LM_j} will depend on time, T_j, ε_j, the shape of the cavity, and constants modeling the porosity of the impregnated medium. Note that the factor(s) T_j are introduced because the liquid moments should vanish when $T_j = 0$. Furthermore, C_{LM_j} causes rotations in the plane of $\exp(i\phi_j)$ as well as rotations out of this plane, and so the following definition is introduced:

$$C_{\mathrm{LM}_j} = C_{\mathrm{LSM}_j} + iC_{\mathrm{LIM}_j} \tag{4}$$

where C_{LSM_j} and C_{LIM_j} are real and represent the liquid side moment and the liquid in-plane moment coefficients, respectively [3].

Combining the payload moment of Eq. (3) with the aerodynamic force and moment produces a slightly more complicated differential equation [3] for $\tilde{\xi}$. Assuming the projectile angular motion continues to be described by an epicycle of Eq. (1) causes the frequency and damping to take the forms

$$T_j = \sigma/2\left[f_j - (-1)^j \sqrt{f_j^2 - 1/S_g}\right] \tag{5}$$

$$\varepsilon_j = \varepsilon_{aj} + C_{\mathrm{LSM}_j}(m_L a^2/I_x)(2T_j/\sigma - 1)^{-1} \tag{6}$$

The last equation shows that C_{LSM_j} has the same effect on damping angular motion as does the aerodynamic damping moment, and the coefficient of C_{LSM_j} being positive for the fast mode means that $C_{\mathrm{LSM}_j} > 0$ will undamp the motion. Similarly, negative C_{LSM_j} will undamp the slow mode.

Equations Governing Liquid Motion

The governing equations describing the flow velocity $\mathbf{V}$ and pressure Q of a low-viscosity liquid are the Euler equations and continuity equation:

$$\rho[\dot{\mathbf{V}} + (\mathbf{V} \bullet \nabla)\mathbf{V}] = -\nabla Q \qquad \nabla \bullet \mathbf{V} = 0 \tag{7}$$

Projectiles considered in this paper have a liquid-saturated porous media payload occupying a cylindrical volume with a diameter of $2a$ and height of $2C$. The cylinder's axis is collinear with the projectile axis, with its center located at the projectile's center of mass. The porous media is assumed to be rigid and rigidly attached to the projectile (see Fig. 1). Continuing with linear theory, the liquid moment is assumed to be generated by the coning or spiral motion of the form

$$\tilde{\beta} + i\tilde{\alpha} = K_j e^{i\phi_j} = \hat{K}_j e^{(\varepsilon + i)TPt} \tag{8}$$

Because the total liquid moment is the sum of moments due to two coning motions, our analysis will consider a projectile subjected to a single coning motion of frequency T and undamping ε. The velocity

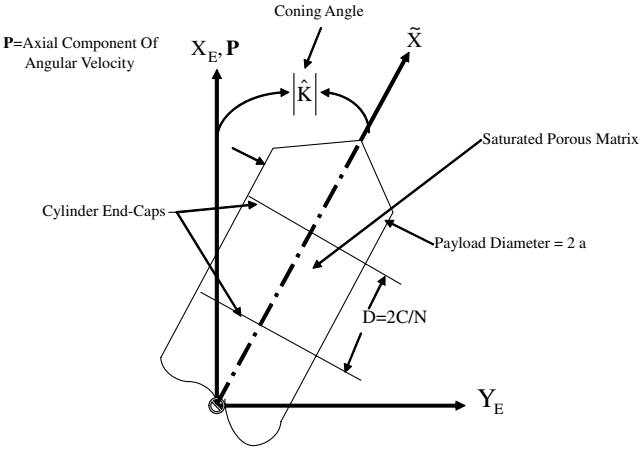

Fig. 1 Configuration coordinate systems and projectile schematic.

for a single coning mode of any point on the projectile will have Earth-fixed cylindrical components [3] given by Eq. (9a):

$$\begin{aligned} V_r &= -xPe^{\varepsilon PTt}[\varepsilon T\cos(PTt - \theta) - (T-1)\sin(PTt - \theta)] \\ V_\theta &= Pr - xPe^{\varepsilon PTt}[\varepsilon T\sin(PTt - \theta) + (T-1)\cos(PTt - \theta)] \\ V_x &= rPe^{\varepsilon PTt}[\varepsilon T\cos(PTt - \theta) - (T-1)\sin(PTt - \theta)] \end{aligned} \tag{9a}$$

where r, θ, and x are cylindrical coordinates in the nonrolling frame. For convenience, these components are written in complex form by introducing the complex frequency $S \equiv (\varepsilon + i)T$:

$$\begin{aligned} V_r &= -\Re(xP(S-i)\hat{K}e^{PSt - i\theta}) \\ V_\theta &= Pr + \Re(ixP(S-i)\hat{K}e^{PSt - i\theta}) \\ V_x &= \Re(rP(S-i)\hat{K}e^{PSt - i\theta}) \qquad \Re(\,) = \text{real part}(\,) \end{aligned} \tag{9b}$$

The liquid velocity $\boldsymbol{q} = (V_r, V_\theta, V_x)$ and pressure $\hat{P}$ are assumed to take a steady-state form, similar to Eq. (9b), so that

$$\begin{aligned} V_r &= \Re(ve^{PSt - i\theta})(Pa) \qquad V_\theta = \Re(we^{PSt - i\theta})(Pa) + rP \\ V_x &= \Re(ue^{PSt - i\theta})(Pa) \qquad \hat{P} = \Re(pe^{PSt - i\theta})(\rho P^2 a^2) + \rho P^2 r^2/2 \end{aligned} \tag{10}$$

where the four small functions v, w, u, and p all depend on r and θ. The Euler equations are modified by additional terms proportional to the relative velocity $\boldsymbol{q} - (S-i)P[-x, ix, r]e^{PSt - i\theta}$ [see Eq. (9b)], to account for inviscid flow in porous media. Substituting Eqs. (10) into the modified version of Eqs. (7) and keeping only the highest-order terms in v, w, and u gives the following linearized equations:

$$\begin{aligned} (S + C_t - i)v - 2w + a\frac{\partial p}{\partial r} &= -\frac{x}{a}C_t(S-i) \\ (S + C_t - i)w + 2v - \frac{iap}{r} &= i\frac{x}{a}C_t(S-i) \\ (S + C_x - i)u + a\frac{\partial p}{\partial x} = \frac{r}{a}C_x(S-i) \qquad \frac{\partial rv}{\partial r} - iw + r\frac{\partial u}{\partial x} &= 0 \end{aligned} \tag{11}$$

where the proportionality constants C_t and C_x represent modifications due to flow in the porous matrix. The porosities in the radial and azimuthal directions, C_t, are identical, but the porosity in the axial direction, C_x, may have a different value. This correction for porous flow stems from Darcy's Law [9,11], where $C_t = \mu/(\rho\kappa_t P)$ and, similarly, $C_x = \mu/(\rho\kappa_x P)$.

Solving the first three equations of Eqs. (10) leads to the velocity field expressions:

$$v = -\frac{2ip - (\mathrm{d}p/\mathrm{d}r)(S + C_t - i)r}{r/a(S + C_t - 3i)(S + C_t + i)} - \frac{x/aC_t(S - i)}{S + C_t + i}$$
$$w = \frac{i(S + C_t - i)p + 2r(\mathrm{d}p/\mathrm{d}r)}{r/a(S + C_t - 3i)(S + C_t + i)} + \frac{ix/aC_t(S - i)}{S + C_t + i} \tag{12}$$
$$u = -\frac{a(\mathrm{d}p/\mathrm{d}x)}{(S + C_x - i)} + \frac{r/aC_x(S - i)}{S + C_x - i}$$

Using these expressions in the fourth equation of Eqs. (11) results in a partial differential equation for the small perturbation p:

$$r^2\frac{\mathrm{d}^2p}{\mathrm{d}r^2} + r\frac{\mathrm{d}p}{\mathrm{d}r} - p - r^2\sigma^2\frac{\mathrm{d}^2p}{\mathrm{d}x^2} = 0$$
$$\sigma^2 = -\frac{(S + C_t - 3i)(S + C_t + i)}{(S + C_t - i)(S + C_x - i)} \tag{13}$$

At this point in the analysis, it is useful to consider the cylindrical payload cavity ranging from $-C \le x \le C$ to consist of an end-to-end sequence of N equal-length Δ cylinders with impenetrable endcaps so that $\Delta = 2C/N$. Normal liquid velocity components at the container walls must agree with Eq. (9b), thus yielding a Fourier–Bessel series [9] solution to Eq. (13):

$$p = \left[e^{-i\theta}\sum_{k\in odd} A_k \cos\left(\pi k\frac{C + x}{\Delta}\right)J_1\left(\frac{\Gamma r}{a}\right) + \left(\frac{rxE}{a^2} + \frac{rD}{a}\right)e^{-i\theta}\right]$$
$$A_j = \frac{16(-1)^n CS(S - i)(S + C_t - 3i)}{\pi^2 ak^2 N(J_1(\Gamma)(S + C_t + i) - \Gamma J_0(\Gamma)(S + C_t - i))}$$
$$\Gamma = \frac{\pi ak\sigma N}{2C} \qquad E = -(S - i)^2$$
$$D = 2C(-N + 2n + 1)(S - i)\frac{S}{Na} \qquad 0 \le n \le N \tag{14}$$

Liquid Moments

The induced liquid moment contained in the segmented cavity is calculated from the time derivative of the angular momentum field. Considering a single coning mode of frequency T, Eq. (3) now gives the transverse liquid moments in the following form:

$$M_{L\tilde{Y}} + iM_{L\tilde{Z}} = T(m_L a^2 P^2)\left[C_{\mathrm{LSM}}\left(T, N, \frac{C}{a}, C_t, C_x\right) + iC_{\mathrm{LIM}}\left(T, N, \frac{C}{a}, C_t, C_x\right)\right]\hat{K}e^{PSt} \tag{15}$$

The induced liquid moment calculated for the entire payload of N end-to-end subcylinders of length Δ is given by

$$TC_{\mathrm{LM}} = -\sum_{n=0}^{N-1}\Re\left\{e^{PSt}\int\frac{\mathrm{R}}{a}\times[((S - i)v - 2w)\mathbf{e_r} + ((S - i)w + 2v)\mathbf{e_\theta} + (S - i)u\mathbf{e_x}]e^{-i\theta}\,\mathrm{d}\Omega\right\}$$
$$\Omega = \pi a^2\Delta \tag{16}$$

for which the velocities are given in Eqs. (12) and the fluctuating part of Eq. (14). Integration of Eq. (16) parallels investigations presented elsewhere [3,9], and so the details will not be given here, but the result is the following expression:

$$TC_{\mathrm{LM}} = \frac{4iC^2(S - i)((N^2 - 1)S^2 + (C_t + 2i)N^2S + (iC_t - 1)N^2)}{3a^2N^2(S + C_t + i)} - \frac{i(3S((4C^2 - a^2)S + 2ia^2) + 16C^2)}{12a^2} - \frac{128iC^2S^2(S - i)(S + C_t - 3i)}{\pi^4N^2a^2(S + C_t + i)} \times\sum_{kodd}\frac{J_1(\Gamma)}{[J_1(\Gamma)(S + C_t + i) - \Lambda J_0(\Gamma)(S + C_t - i)]k^4}$$
$$\Gamma \equiv \pi k\sigma Na/2C \tag{17}$$

Severe flight instability can occur whenever S has a value so that

$$J_1(\Gamma)(S + C_t + i) - \Gamma J_0(\Gamma)(S + C_t - i) \approx 0 \tag{18}$$

Familiar examples are the Stewartson [1] eigenvalues, which exist when $C = C_x = 0$, and a good discussion of these for projectiles with liquid payloads is found in Murphy [3]. Eigenvalues for $C_t \ne 0$ and $C_x \ne 0$ require a numerical search procedure in the complex plane.

Limiting values of Eq. (17) as the number of cylinders N becomes large shows that C_{LM} approaches a value such that

$$\lim_{N\gg 1} C_{\mathrm{LSM}} = \frac{\varepsilon}{2}\left[1 - T\frac{4C^2/a^2 + 3}{3}\right] \equiv C_{\mathrm{LSM}_F}$$
$$\lim_{N\gg 1} C_{\mathrm{LIM}} = \frac{1}{2} + \frac{(4C^2/a^2 + 3)}{12}T(\varepsilon^2 - 1) \equiv C_{\mathrm{LIM}_F} \tag{19}$$

These values are the same as those caused by a liquid with infinite viscosity [3,9] and are therefore referred to as *frozen liquid values*. Please note that [3] ignores the ε^2 term, because ε is typically small.

Results

Scheidegger [12] has tabulated permeabilities for hair felt with porosity $\kappa \cong 1.0 \times 10^{-5}$ cm^2 and (assuming the media studied here has similar permeabilities) says that, on average, $0 < C_t$ and $C_x < 5$. The most important results concerning the designer are the liquid side moments; hence, the presentation will focus on the side moment coefficient C_{LSM} over a typical range of coning frequencies T. Figure 2 gives examples of C_{LSM} for two end-to-end cylinders as functions of the coning frequency T with fixed values of C_t and C_x and a range of ε values. The corresponding liquid side moment can be determined by multiplying these results with $m_L P^2 a^2$ of the particular liquid and total axial spin of the projectile.

A design feature that may be important is to let the porosity in the axial direction be different than porosities in the orthogonal directions. The influence of letting the axial porosity C_x change for a given value of C_t is shown in Fig. 3, depicting a single cylindrical cavity of aspect ratio 2 undergoing coning motion with a prescribed undamping. This figure shows that differences in the porosities C_t and C_x can have a significant impact on the liquid side moment.

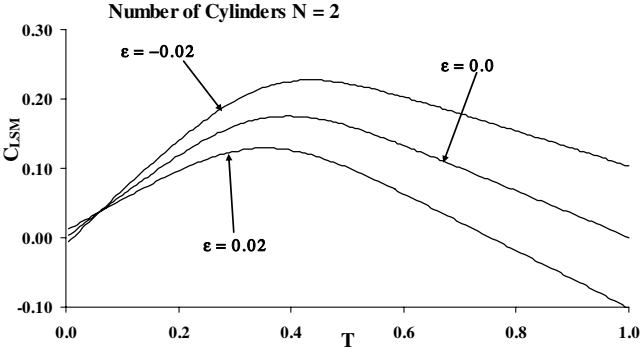

Fig. 2 C_{LSM} **vs coning frequency** T.

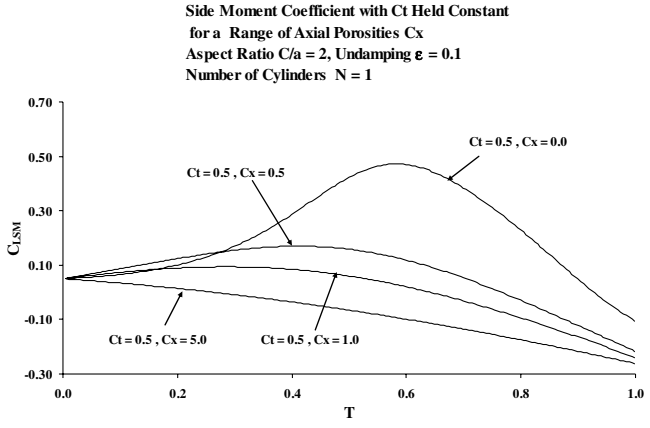

Fig. 3 C_{LSM} vs coning frequency T.

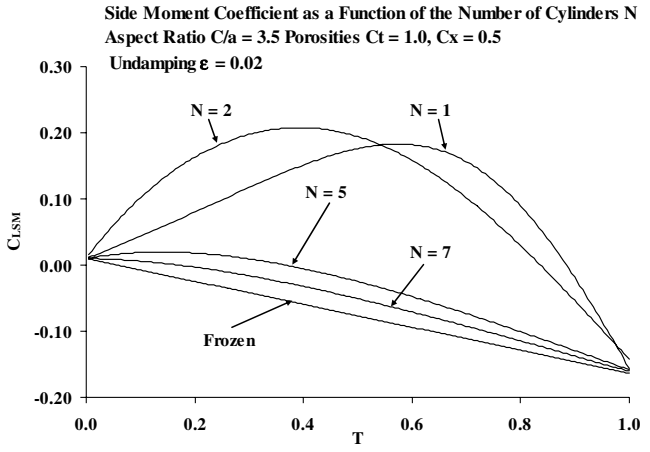

Fig. 4 C_{LSM} vs coning frequency T approaching frozen liquid values.

Plots showing the liquid moment coefficient C_{LSM} progressing toward the frozen liquid value C_{LSM_F} [Eqs. (19)] as the number of cylinders in the payload stack increases are presented in Fig. 4. Evidently, a payload consisting of enough end-to-end cylinders with impermeable endcaps behaves like a liquid payload having infinite viscosity [3]. This means that with a sufficient number of cylinders N, the side moment caused by a liquid payload can be determined from the first equation of Eqs. (19).

As already mentioned, Eq. (18) has Stewartson [1] solutions when $C_t = C_x = 0$. The effect of one such solution, $T = 0.3324$, $\varepsilon = 0.0000$, $C/a = 1.5$, $k = 3$, and $N = 1$, is given by the $C_t = C_x = 0$ line in Fig. 5 and to avoid an infinite liquid side moment $\varepsilon = 0.02$ for this line. Using nonzero values of porosity $C_t = C_x = 0.1$ can greatly reduce the resonant effect for the same value of undamping $\varepsilon = 0.02$, as shown in Fig. 5. However, including a porous matrix will generally shift the eigensolution off of the real axis, and so the solution to Eq. (18) now becomes $T = 0.3324$, $\varepsilon = -0.3008$, $C/a = 1.5$, $k = 3$, and $N = 1$. The $C_t = C_x = 0.1$, $\varepsilon = -0.3000$ line in Fig. 5 shows this resonant response in which (again to avoid infinite values of C_{LSM}) undamping is now taken to be $\varepsilon = -0.3000$. Thus, one way to avoid severe flight instabilities is to adjust the porosities of the matrix and/or the aspect ratio of the liquid payload to move the solutions of Eq. (18) out of the operational range of the given projectile.

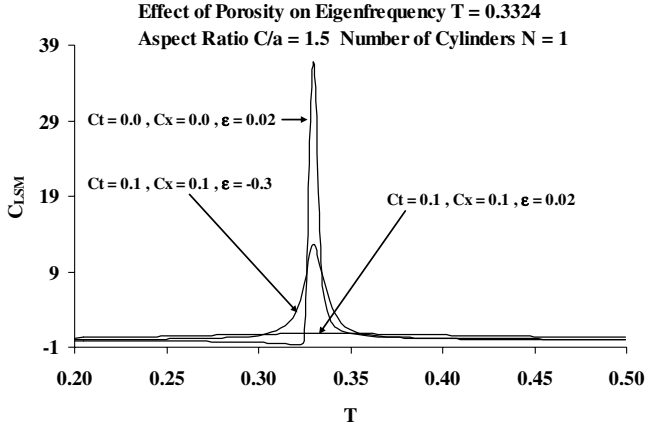

Fig. 5 C_{LSM} vs coning frequency T, showing an example of a Stewartson eigenfrequency shift.

Conclusions

Liquid moment coefficients are computed for coning projectiles with a segmented stack of cylindrical cavities filled with a permeable medium, each fully impregnated with an inviscid liquid. The moment coefficients C_{LSM} and C_{LIM} enable an investigator to calculate liquid moments induced by a given liquid undergoing projectile coning motion described by angular velocity P. The most important moment is the liquid side moment, proportional to C_{LSM}, because that moment can cause flight stability problems. C_{LSM} is presented as functions of coning frequency, fineness ratio, and constants C_t and C_x, used to represent porosity in the transverse and axial directions of the permeable medium. Differences between the axial porosity C_x and transverse porosity C_t can produce significant changes to the liquid side moment. As the number of segmented cylinders containing the saturated liquid payload increases, the liquid side moment approaches the value it would have if the liquid were frozen.

The presence of permeable media causes the familiar Stewartson [1] inviscid eigenfrequencies to migrate off the real axis into the complex plane. This may help the designer avoid resonances that can cause destabilizing liquid side moments on a coning projectile. The more familiar way to avoid resonances is to adjust the aspect ratio of the liquid cavity, which can still be done with the inclusion of porous media.

Most spin-stabilized projectiles exhibit angular motion that is well-approximated by the sum of fast and slow coning motions. One way to include liquid payload contributions in a six-degree-of-freedom analysis is to consider Eq. (3). Here, the liquid moments $M_{L\tilde{Y}} + iM_{L\tilde{Z}}$ are represented in the nonrolling frame, and the phase factor e^{iT_jPt} suggests interpreting $m_L a^2 P^2 T_j C_{\mathrm{LM}_j} K_j$ as an average liquid moment contribution in the body frame.

References

[1] Stewartson, K., "On the Stability of a Spinning Top Containing Liquid," *Journal of Fluid Mechanics*, Vol. 5, No. 4, Sept. 1959, pp. 577–592. doi:10.1017/S0022112059000404

[2] Wedemeyer, E. H., "Viscous Correction to Stewartson's Stability Criterion," U.S. Army, Ballistic Research Labs., Rept. 1325, Aberdeen Proving Ground, MD, June 1966.

[3] Murphy, C. H., "Angular Motion of a Spinning Projectile with a Viscous Liquid Payload," *Journal of Guidance, Control, and Dynamics*, Vol. 6, No. 4, July–Aug. 1983, pp. 280–286.

[4] Gerber, N., Sedney, R., "Moment on a Liquid-Filled Spinning and Nutating Projectile: Solid Body Rotation," U.S. Army, Ballistic Research Labs., TR-02470, Aberdeen Proving Ground, MD, Feb. 1983.

[5] Hall, P., Sedney, R., and Gerber, N., "Fluid Motion in a Spinning, Coning Cylinder via Spatial Eigenfunction Expansion," U.S. Army, Ballistic Research Labs., BRL-TR-2813, Aberdeen Proving Ground, MD, Aug. 1987.

[6] Mohamed, S., Rihua, L., and Herbert, Th., "Eigenfunction Expansion of the Flow in a Spinning and Nutating Cylinder," *Physics of Fluids A* Vol. 4, No. 9, Sept. 1992, pp. 1998–2007. doi:10.1063/1.858369

[7] D'Amico, W. P., and Mark, A., "The Application of a Highly Permeable Medium to Reduce Spin-Up Time and to Stabilize a Liquid-Filled Shell," U.S. Army, Ballistic Research Labs., MR-02851, Aberdeen Proving Ground, MD, July 1978.

[8] D'Amico, W. P., and Clay, W. H., "Flight Tests for Prototype Felt Wedge/White Phosphorous Improved Smoke Concept," U.S. Army, Ballistic Research Labs., MR-02824, Aberdeen Proving Ground, MD, Apr. 1978

[9] Cooper, G. R., "Moment Exerted on Coning Projectile by a Spinning Liquid in a Cylindrical Cavity Containing a Porous Medium," U.S. Army, Ballistic Research Labs., MR-3677, Aberdeen Proving Ground, MD, June 1988.
[10] Murphy, C. H., "Free Flight Motion of Symmetric Missiles," U.S. Army, Ballistic Research Labs., Rept. 1216, July 1963.
[11] Darcy, H., "Les Fontaines Publiques de la Ville de Dijon," Dalmont, Paris, 1856.
[12] Scheidegger, A. E., *The Physics of Flow Through Porous Media*, Univ. of Toronto Press, Toronto, 1960.

R. Rangel
Associate Editor